# Chemical bonding in the lightest tri-atomic clusters; $H_3^+$, $Li_3^+$ and $B_3^-$

**ARTICLE** *in* JOURNAL OF MOLECULAR STRUCTURE THEOCHEM · MAY 2009

Impact Factor: 1.37 · DOI: 10.1016/j.theochem.2009.02.003



**2 AUTHORS:**

Cina Foroutan-Nejad
Masaryk University
**29** PUBLICATIONS **243** CITATIONS
SEE PROFILE

Parviz Rashidi
University of Tehran
**52** PUBLICATIONS **377** CITATIONS
SEE PROFILE

Journal of Molecular Structure: THEOCHEM xxx (2009) xxx–xxx

Contents lists available at ScienceDirect

Journal of Molecular Structure: THEOCHEM

journal homepage: www.elsevier.com/locate/theochem

# Chemical bonding in the lightest tri-atomic clusters; $H_3^+$, $Li_3^+$ and $B_3^-$

Cina Foroutan-Nejad, Parviz Rashidi-Ranjbar *

*School of Chemistry, University College of Science, University of Tehran, Enghelab Avenue, Tehran 1455-64155, Iran*

ARTICLE INFO

*Article history:*
Received 15 October 2008
Received in revised form 1 February 2009
Accepted 2 February 2009
Available online xxxx

*Keywords:*
$H_3^+$
$Li_3^+$
$B_3^-$
Atomic clusters
QTAIM

ABSTRACT

Detailed topological charge density analysis and the Quantum Theory of Atoms in Molecules (QTAIM) calculations has been performed on equilibrium geometries of the three lightest tri-atomic clusters; $H_3^+$, $Li_3^+$ and $B_3^-$. Characteristics of critical points of charge density, the effects of occupied molecular orbitals on topology of charge density, the stability of molecular graphs toward nuclear excursions and the QTAIM integration results were used to draw a picture of bonding in these clusters. Topological networks in $H_3^+$ and $B_3^-$ are unstable but molecular graph of $Li_3^+$ is stable under finite geometry changes. $H_3^+$ is best represented as a 3-membered ring; lithium atoms in $Li_3^+$ surround the electrons in basin of a Non-Nuclear Maximum (NNM) by an electrostatic interaction; and in $B_3^-$ an extended bonding pattern was found.



## 1. Introduction

Exploring the electronic structure and bonding pattern of small clusters have always been fascinating for both experimental and theoretical chemists.

The present account concerns with both topological analysis of charge density and the "Quantum Theory of Atoms in Molecules" QTAIM, [1,2] investigation of $H_3^+$, $Li_3^+$ and $B_3^-$, the three lightest atomic clusters with a "Non-Nuclear Maxima" (NNM) in their charge density. The NNM of charge density or pseudo atom is known both experimentally and theoretically [3–13]. It has been suggested that appearance of a NNM is a normal stage in the formation of a chemical bond in homo-nuclear diatomic molecules, but only for an appropriate and usually narrow, range of inter-nuclear distances. For most elements, however, this range occurs far away from the equilibrium geometry in the gas phase or those under normal thermodynamic conditions [13].

The energy and charge of the basin of NNM (the pseudo atom) are usually obtained by subtracting the sum of energy and charge of the other atoms (obtained by the QTAIM analysis) from the total electronic energy and charge of molecules, calculated by ab initio or DFT methods. Properties of the NNM have been studied individually in a few cases [11,12].

In this paper properties of the NNM (pseudo atom) are computed by insertion of a ghost atom, Bq, in the basin of pseudo atom. The electron delocalization indices $\delta(x, y)$ [1,14] between the basins of atoms around the NNM are evaluated and compared with delocalization indices between pseudo atom and the surrounding atoms to draw a chemical picture of bonding for the considered species. Topological analysis of charge density is also employed to obtain a parallel picture of bonding in these species for comparison with results obtained from QTAIM analysis.

According to this study, three different bonding patterns are emerged for $H_3^+$, $Li_3^+$ and $B_3^-$.

## 2. Computational details

All structures were optimized at the RB3LYP and the RCCSD levels of theory with the cc-pVTZ and the aug-cc-pVTZ basis sets implemented in the Gaussian 98 suite of programs [15]; $D_{3h}$ minimum energy structures with no imaginary frequencies were obtained for all considered molecules. Electron densities were analyzed by the AIM2000 program [16]. Non-Nuclear Maxima (NNM), coinciding with (3, −3) critical points [1], were found in the centers of all species at all computational levels. Electron densities derived from the four levels of calculations were analyzed further and the Molecular Graphs (MG) [1] of molecules were obtained. Results of the topological analysis of charge density at the RB3LYP/aug-cc-pVTZ level of theory are gathered in Table 1 and Table S-1. Fig. 1 shows basins of NNM (pseudo atoms) and the surrounding atoms at equilibrium geometries. All results in this paper are presented at the RB3LYP/aug-cc-pVTZ level of theory. This level is chosen because augmented basis sets are more successful in describing characteristics of anions. On the other hand localization and delocalization indices are valid only for wave functions which are obtained from the single determinant levels of theory like HF or various DFT methods. Results of the other levels of theory are available in the Supplementary information.

* Corresponding author. Tel.: +98 21 66495291; fax: +98 21 66405141.
*E-mail address:* ranjbar@khayam.ut.ac.ir (P. Rashidi-Ranjbar).

0166-1280/$ - see front matter © 2009 Elsevier B.V. All rights reserved.
doi:10.1016/j.theochem.2009.02.003

**Table 1**
Characteristics of critical points in electron density. $\rho$ is electron density, $\nabla^2\rho$ is the Laplacian of electron density, $H$ is energy density, $G$ is Lagrangian kinetic energy and $\varepsilon$ is ellipticity.

| | $\rho$ | | $\nabla^2\rho$ | $H$ | $G$ | $G/\rho$ | $\varepsilon$ | $\rho(3,-3)/\rho(3,-1)$ |
|---|---|---|---|---|---|---|---|---|
| $H_3^+$ | BCP | 0.2375 | −0.9132 | −0.2283 | 0.0000 | 0.0000 | 1.9015 | 1.0013 |
| | NNM | 0.2378 | −0.9168 | −0.2292 | 0.0000 | 0.0000 | – | |
| $Li_3^+$ | BCP | 0.0143 | 0.0072 | −0.0021 | 0.0039 | 0.2727 | 0.4406 | 1.1469 |
| | NNM | 0.0164 | −0.0116 | −0.0029 | $1.75 \times 10^{-5}$ | | 0.0011 | – |
| $B_3^-$ | BCP | 0.1903 | −0.2028 | −0.1954 | 0.1447 | 0.7604 | 1.0733 | 1.0215 |
| | NNM | 0.1944 | −0.2280 | −0.1488 | 0.0712 | 0.3663 | – | |

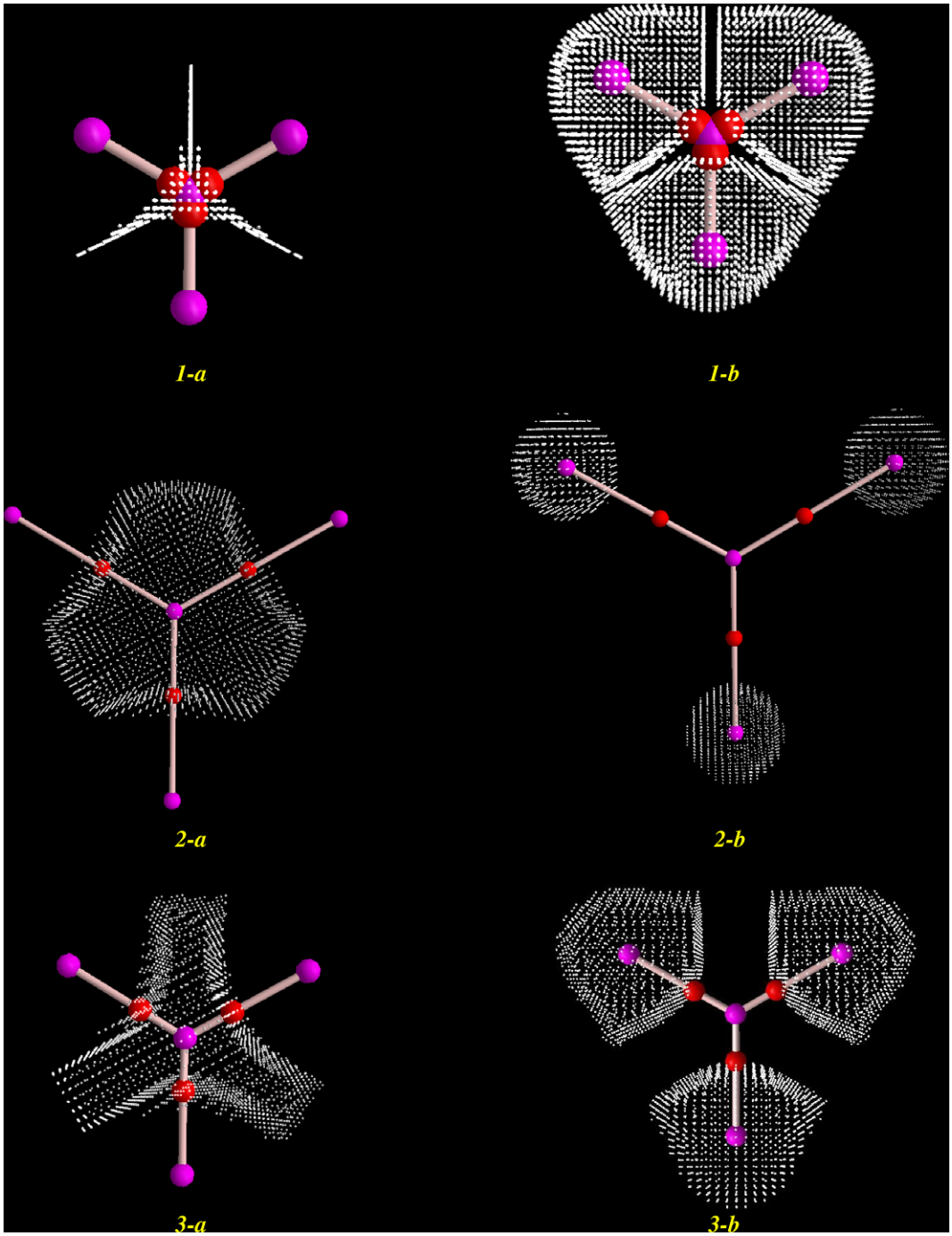


**Fig. 1.** Basin of non-nuclear attractors (a) and atomic nuclei (b) in $H_3^+$ (1), $Li_3^+$ (2) and $B_3^-$ (3). Purple dots are (3, −3) critical points, nuclear and non-nuclear attractor, red dots are (3, −1) critical points. (For interpretation of the references to colour in this figure legend, the reader is referred to the web version of this article.)

Please cite this article in press as: C. Foroutan-Nejad, P. Rashidi-Ranjbar, J. Mol. Struct. (THEOCHEM) (2009), doi:10.1016/j.theochem.2009.02.003

If a MG derived from the topological analysis of charge density does not change for a finite domain of geometrical changes, it is called a stable MG [1]. It means that the number and the type of critical points remain unchanged when the positions of the nuclei are altered due to molecular vibrations. On the other hand, in a typical chemical reaction, MG of reactants change to MG of products by transition from an unstable MG. Unstable Molecular Graphs are classified into two distinct groups. The first class has been named bifurcation topological network; this type of MG is distinguishable by critical points with ranks lower than three or the so-called degenerate critical points and the other class contains networks with critical points whose connection causes the "non-transverse" intersect of stable and unstable manifolds, this class of unstable MG are called conflict structures [1].

To examine the stability of topological patterns regarding the nuclear excursions, the distances between the NNM and the nuclei were increased by up to 15% of their equilibrium distance in each species; first for one atom, then for two atoms and finally for all three atoms surrounding the NNM. Characteristics of the critical points (CP) of electron density were investigated to determine the bonding nature of the species. The electron density $\rho_b$ at the (3, −1) critical points or bond critical point (BCP) is a criterion of bonding in the topological analysis of charge density, and its large values indicate shared interactions [1,14]. The Laplacian of electron density at the BCP, $\nabla^2\rho_b$, is another criterion of bonding. Its negative values indicate charge concentration which implies shared interactions while its positive values indicate charge depletion which implies closed shell interactions (shared and closed shell interactions often coincide with the covalent and ionic bonds in the VB terminology, respectively) [1,14]. The energy density $H_b$, negative of the Hamiltonian kinetic energy, is negative for shared bonds and positive for closed shell interactions. The ratio of $G_b/\rho_b$ where $G_b$ is the Lagrangian kinetic energy density at the (3, −1) critical point is another criterion of bonding. It places the dominance of kinetic energy density on an absolute scale; values greater than 1.0 imply closed shell interaction while values less than 1.0 imply shared interactions [1,14]. The ellipticity of a bond, $\varepsilon$, is defined as $\varepsilon = \lambda_1/\lambda_2 - 1$ where $\lambda_1$ and $\lambda_2$ are two negative eigenvalues of the Hessian matrix of charge density and $\lambda_2$ is the smaller curvature by convention. Ellipticity provides the measure of the extent that the charge density is preferentially accumulated in a given plane. It has been interpreted as the presence of π interaction between atoms in stable MG, but it usually indicates instability in MG [1].

To find the role of each molecular orbital (MO) in total charge density of $Li_3^+$ and $B_3^-$, the electrons were removed from the HOMOs (derived from calculations at the RB3LYP with both the cc-pVTZ and the aug-cc-pVTZ basis sets), respectively, and variations in the electron density of $Li_3^+$ and $B_3^-$ were probed.

The energy and charge were calculated for each atom and the NNM. Results of the QTAIM calculations are compared with those of the DFT calculations in Table S-2 (Supplementary information). Accuracy of the QTAIM calculations is satisfactory as the largest error in these calculations is only 0.62 kcal $mol^{-1}$.

The electron delocalization index, $\delta(x, y)$ is the measure of the extent that electrons in the basin of one atom are exchanged with electrons in the basin of another atom. The delocalization index is a quantitative measure of covalency in homo-nuclear molecules [1,14] which can be measured between any pair of atoms. It does not depend on the presence of (3, −1) critical points and is an individual criterion of bonding. Recently, Farrugia et al. found a certain case in which several bonding criteria including delocalization index, were predicting that a chemical bond is present but no (3, −1) critical point was found between bonded atoms; they have proposed that the delocalization index is a more reliable criterion of bonding in the context of QTAIM than the presence of (3, −1) critical points [17]. In the present paper, the bonding pattern of all studied species are depicted concerning the delocalization index rather than the characteristics of the (3, −1) critical points.

The localization index, $\lambda_{(x)}$ of atom X, is the number of electrons which are localized in the basin of that atom and the percent localization index, $l_{(X)}$, of the atom X is defined as $l_{(x)} = \lambda_{(x)}/N_{(x)} \times 100$ where $\lambda_{(x)}$ is the localization of the atom X and $N_{(x)}$ is the number of electrons in the basin of that atom, $N_{(x)}$ in NNM are equal to their charge, $q$, since there is no nucleus in the basin of NNM. The percent localization index approaches 100 in closed shell interactions [14].

## 3. Results and discussion

### 3.1. $H_3^+$

Since it's first observation by Thomson in 1911, [18,19] $H_3^+$ has raised interest of many scientists [20–31]. This molecule is an ideal target for computational and theoretical chemists. A number of theoretical papers dealing with different aspects of electronic, vibration–rotational spectral properties and details of the ground state potential energy surface (PES) within micro hartree limit have been published on $H_3^+$ since mid seventies. Carney and Porter have performed the first ab initio calculations and computed the bond length, vibrational and rotational spectra of $H_3^+$ [32–34]. This subject has been revised by different authors [35–40]. The PES of $H_3^+$ at its equilibrium configuration has been calculated by bare nuclear Hamiltonian [36]. The vibrational term values for the fundamental bands and some overtones of $H_3^+$ with maximum of 0.5 $cm^{-1}$ error compared to experimental values have been calculated [37]. Accuracy of Born–Oppenheimer PES of $H_3^+$ has been reached 0.02 $cm^{-1}$ (0.1 micro Hartree) [38]. Rovibrational frequencies of $H_3^+$ has been later calculated with residual discrepancies of a few tenth of $cm^{-1}$ [39] and by fitting surfaces to the Born–Oppenheimer potential energy, electronic relativistic correction and adiabatic correction data; calculations have reproduced the known spectroscopic data of the molecule and its isotopomers to within a few hundredths of a wave number ($cm^{-1}$) [40].

The topology of charge density of $H_3^+$ based on the QTAIM analysis is discussed in a few papers [1,41–43]. The MG of $H_3^+$ derived from the topological analysis of charge density by the QTAIM depends on method and/or basis set. The NNM was not found in the early studies [41,42]; but it was found later at the HF/cc-pVQZ level of theory [43]. Based on the topological analysis of charge density it has been suggested that the structure of $H_3^+$ is not a ring [43]. However, it has been shown that a ring current similar to known aromatic compounds does exists in $H_3^+$ [44].

The electron density of $H_3^+$ is studied carefully in this work. Every atom in $H_3^+$ is 0.370 au positively charged and −0.111 au charge is accumulated in the basin of pseudo atom (NNM) at the center of molecule. Electron localization in each hydrogen nucleus basin and the basin of NNM (pseudo atom) are 0.1982 au and 0.0062 au, respectively (Table 2). This means that almost all electrons are delocalized between basins of hydrogen nuclei and there is approximately no localized electron in the basin of pseudo atom.

**Table 2**
Integrated basin energy $E$ (Ω), in atomic unit, electric charge $q$ (Ω), electron localization $\lambda$ (Ω), delocalization $\delta(x, y)$ indices and energy per electron $E$ (Ω)/$N$ (Ω).

| | | $E$ (Ω) | $q$ (Ω) | $\lambda$ (Ω) | $\delta(x, y)$ | $E$ (Ω)/$N$ (Ω) |
|---|---|---|---|---|---|---|
| $H_3^+$ | H | −0.433352 | 0.370 | 0.1982 | 0.3963 | |
| | NNM | −0.047277 | −0.111 | 0.0062 | 0.0699 | −0.425919 |
| $Li_3^+$ | Li | −7.410987 | 0.820 | 2.0121 | 0.0344 | |
| | NNM | −0.142050 | −1.450 | 1.0410 | 0.2715 | −0.097966 |
| $B_3^-$ | B | −24.437512 | 0.503 | 3.0874 | 0.8687 | |
| | NNM | −1.091029 | −2.508 | 0.8838 | 1.0784 | −0.434950 |

Please cite this article in press as: C. Foroutan-Nejad, P. Rashidi-Ranjbar, J. Mol. Struct. (THEOCHEM) (2009), doi:10.1016/j.theochem.2009.02.003

The delocalization index between the hydrogen nuclei basins is 0.3963 au and between the hydrogen nuclei basins and the basin of pseudo atom is 0.0699 au. This demonstrates that delocalization between pseudo atom and each hydrogen nuclei is equal to 63% of electron density of pseudo atom. Characteristics of the (3, −3) critical point in $H_3^+$ (NNM) and (3, −1) critical points between the NNM and hydrogen nuclei are listed in Table 1. Electron density at the (3, −3) critical point (NNM) is very similar to electron density at the (3, −1) critical points between the NNM and hydrogen nuclei. The ratio of $\rho(3,-3)/\rho(3,-1)$ is only 1.0013, which indicates the flatness of charge density at the center of $H_3^+$. Moreover, the electron density $\rho_b$ (0.2375), the Laplacian of electron density $\nabla^2\rho_b$ (−0.9132), the energy density $H_b$ (−0.2283), and the ratio of Lagrangian kinetic energy density to electron density, $G_b/\rho_b$ (0.0000) are similar to the characteristics of a pure shared interaction.

The volume per electron is calculated in both basins which shows that charge in the basin of pseudo atom is more condensed compared to the charge in the basin of hydrogen nuclei Table 3.

Ellipticity defined in the (3, −1) critical points is considerably high (1.9015); large values of ellipticity are usually observed in conflict structures. This large value indicates that a small change in the position of one of nuclei may change the topology of charge density of molecule considerably as have been proven previously for other molecules with unstable MG [45].

Increasing the distance between one hydrogen nucleus and the NNM changes the molecular graph to the conflict structure [42], Fig. 2(1-a), in which two (3, −1) critical points are connected to each other by a bond path. By increasing distances of two hydrogen atoms, the NNM vanishes again, Fig. 2(1-b). But increasing distances of three hydrogen atoms symmetrically even by 15% of bond path length does not affect the presence of the NNM Fig. 2(1-c).

The percent localization in the basin of NNM in $H_3^+$ is 5.59% of its population. Similarly the percent localization in basin of hydrogen nuclei is 31.48%, see Table 3.

All topological characteristics of $H_3^+$ are indicating the presence of shared interaction. The electron delocalization between basins of the hydrogen nuclei is proportionally high, indicating considerable degree of covalency.

Studying the topology of charge density and the delocalization indices among the hydrogen atoms themselves, and between the hydrogen atoms and the NNM suggests that the chemical picture of $H_3^+$ is very similar to a classical ring. This is consistent with the picture obtained from analysis of current density of $H_3^+$.

### 3.2. $Li_3^+$

Lithium clusters, crystals and compounds are studied frequently [11–13,46]. Recently, aromaticity of $Li_3^+$ has been discussed [44,47]. Current density maps obtained by Havenith et al. [44] did not show ring current in this cluster. Topological analysis of charge density of $Li_3^+$ shows a system composed of three lithium atoms bonded to a NNM at the center of this cluster very similar to the topological picture of charge density of $H_3^+$. QTAIM calculations can help unveil the nature of bonding in $Li_3^+$.

The lithium atoms are positively charged by 0.820 au and an electronic charge of −1.450 au is accumulated in the basin of pseudo atom at the center of the molecule, Table 2. Electron localizations of the lithium atom basins (2.0121 au) and the basin of pseudo atom (1.0410 au) are high compared to $H_3^+$. The delocalization index between lithium atoms $\delta$ (Li, Li) is 0.0344 au. The delocalization index between lithium atoms and the basin of pseudo atom, $\delta$ (Li, NNM) is 0.2715 au, Table 2. The percent localization in the basin of pseudo atom of $Li_3^+$ is 71.79%, Table 3, which compared to $H_3^+$ means that $Li_3^+$ is more like an ionic system. The percent localization of lithium atoms in this cluster is 92.19%, consistent with the ionic nature of bonding in the molecule.

The charge in the basin of pseudo atom in $Li_3^+$ is very diffuse, the volume of this basin (295.48 $au^3$) and the volume per electron (203.78 $au^3/e$) are very large (Table 3). This large basin is not affected by increasing the distance between the lithium nuclei and the NNM by up to 15% of their equilibrium distance Fig. 2(2-a to 2-c).

The characteristics of critical points in topology of charge density of $Li_3^+$ are listed in Table 1. Electron density of (3, −1) and (3, −3) critical points are lower than their counterparts in $H_3^+$, but the ratio of $\rho(3,-3)/\rho(3,-1)$ (1.1469) is higher compared to $H_3^+$. This demonstrates that electron density is relatively more localized [12] and the charge density in the center of $Li_3^+$ is less flat. The sign of $\nabla^2\rho$ changes from the (3, −1) critical point (0.0072) to the (3, −3) critical point (−0.0116), although the electron density of (3, −3) critical point is not so high. The energy density in both (3, −1) and (3, −3) critical points are comparable but the Lagrangian kinetic energy density and the ratio of $G/\rho$ varies dramatically from (3, −1) to (3, −3) critical point, Table 1.

By removing two electrons from HOMO in $Li_3^+$, NNM disappears and a (3, +1) or ring critical point is formed in the center of cluster and the electron density of the newly formed critical points decreases dramatically, Scheme S-1. The ratio of $\rho(3,-1)/\rho(3,+1)$ in the new molecule equals to 3.3333. This demonstrates that removing the valence electrons of this cluster, reduces the floppy nature of electron density.

Based on the QTAIM and topological analysis of charge densities, charge is localized in $Li_3^+$ both in the basin of lithium atoms and in the basin of voluminous pseudo atom (NNM). Low electron delocalization between the basins of lithium atoms denies the presence of covalent bonding between them. On the other hand, bonding criteria based on the topological analysis of charge density and behavior of voluminous and topologically stable pseudo atom in $Li_3^+$ are leading to the presence of a kind of closed shell interaction between three lithium ions and their free valence electrons that is manifested in the flatness of charge density and formation of the pseudo atom.

### 3.3. $B_3^-$

$B_3^-$ is the lightest covalently bound cluster with both σ and π bonds according to orbital morphology [48,49]. But the molecular graph of $B_3^-$ obtained from the topological analysis of charge density is similar to the molecular graphs of $H_3^+$ and $Li_3^+$ at first glance. To obtain more insight about the nature of bonding in this cluster, QTAIM and topological analysis of charge density were performed.

Each boron atom in $B_3^-$ is positively charged by 0.503 au and the electronic charge of −2.508 au is accumulated in the basin of pseudo atom. $\lambda$(B), the localization of the basin of boron atoms is 3.0874 au and $\lambda$(NNM) is 0.8838 au, Table 2. The delocalization index between boron atoms $\delta$ (B, B) is 0.8687 au and the delocalization index between the basin of pseudo atom and boron atoms $\delta$ (B, NNM) is 1.0784 au Table 2. The percent localization of the basin of

**Table 3**
Integrated basin properties; volumes in atomic units Vol (Ω), electron density $N$ (Ω), average volume per electron Vol (Ω)/$N$ (Ω), and percent localization $l$ (Ω) calculated by analyzing electron density of DFT(B3LYP/aug-cc-pVTZ).

| | | Vol (Ω)[a] | $N$ (Ω) | Vol (Ω)/ $N$ (Ω) | $l$ (Ω) |
|---|---|---|---|---|---|
| $H_3^+$ | H | 30.34 | 0.6296 | 48.19 | 31.48 |
| | NNM | 3.54 | 0.1110 | 31.89 | 5.59 |
| $Li_3^+$ | Li | 55.34 | 2.1825 | 25.35 | 92.19 |
| | NNM | 295.48 | 1.4500 | 203.78 | 71.79 |
| $B_3^-$ | B | 172.11 | 4.4972 | 38.27 | 68.65 |
| | NNM | 94.38 | 2.5084 | 37.63 | 35.23 |

[a] Atomic volume is calculated in a 0.001 electric charge isosurface.

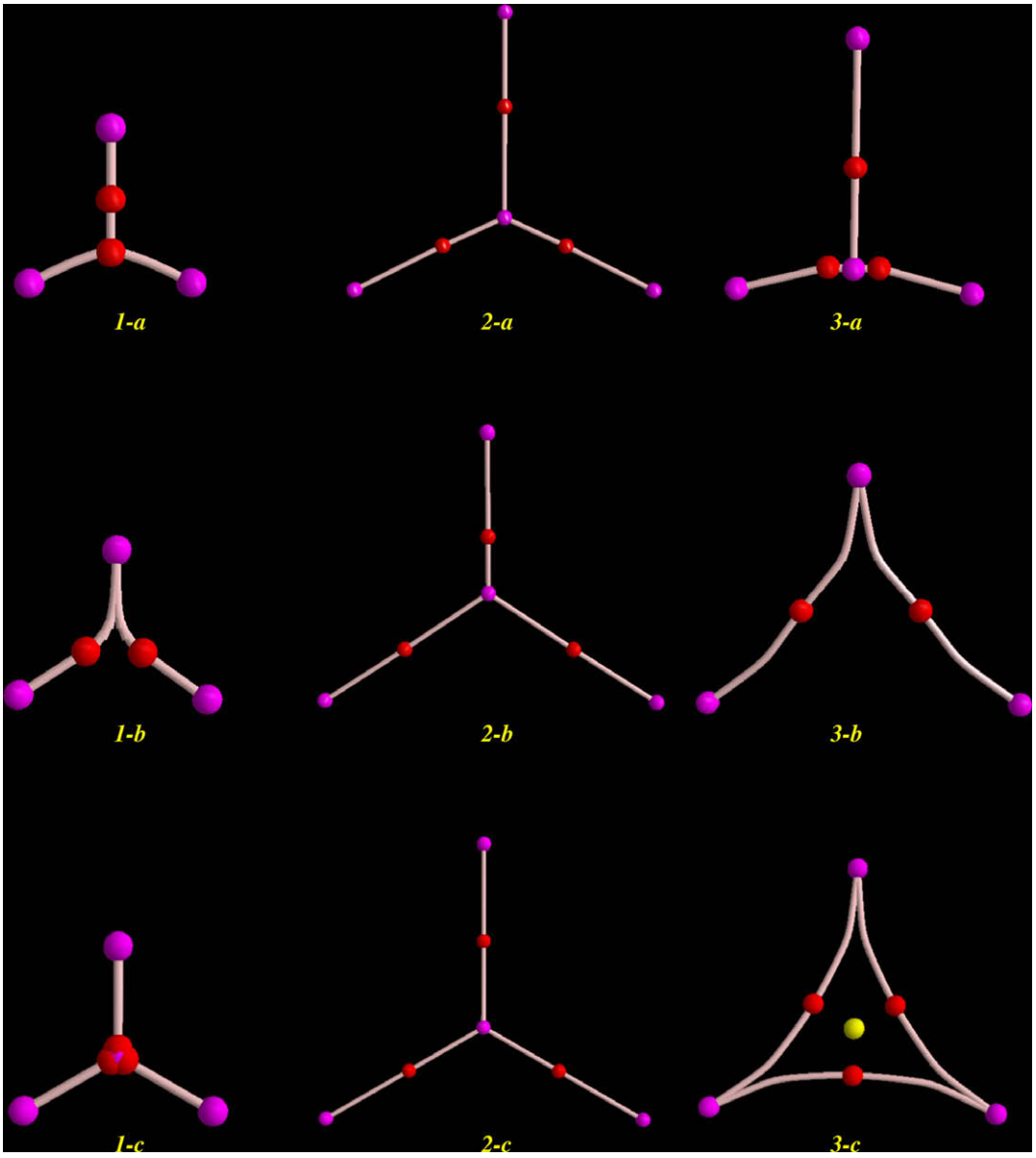


**Fig. 2.** Molecular graphs of $H_3^+$ (1), $Li_3^+$ (2) and $B_3^-$ (3); (a) after increasing the distance between one nucleus and the NNM by 15% of their equilibrium distance (b) after increasing the distances between two nuclei and the NNM by 15% of their equilibrium distances and (c) after increasing the distances between all nuclei and the NNM by 15% of their equilibrium distances, purple dots are (3, −3) critical points, nuclear and non-nuclear attractors and red dots are (3, −1) critical points. (For interpretation of the references to colour in this figure legend, the reader is referred to the web version of this article.)

pseudo atom in $B_3^-$ is 35.23% and that of the boron atoms is 68.65%, Table 3.

The volumes per electron of the basin of pseudo atom (37.63) and the basin of boron atoms (38.27) are similar Table 3. This indicates the floppy nature of charge density in this cluster. Increasing the distance between one atom and the NNM does not affect the presence of NNM Fig. 2(3-a), but increasing the distances of two nuclei from the NNM changes the molecular graph and the NNM vanishes, Fig. 2(3-b). By increasing distances of all three boron atoms from NNM, the (3, −3) critical point at the center of molecule changes to a (3, +1) critical point or ring critical point Fig. 2(3-c).

Analyzing the topology of charge density of this cluster vividly illustrates the floppy nature of charge density. Characteristics of (3, −1) critical points of charge density are within the range of shared interaction, Table 1. The ratio of $\rho(3, -3)/\rho(3, -1)$ is 1.0215 which indicates that charge density is almost equally distributed at the center of the cluster. Surprisingly, removing electrons from HOMO to HOMO-4 does not change this situation, Scheme S-2. In all cases the values of $\rho(3, -3)$, $\rho(3, -1)$ or $\rho(3, +1)$ are very close to each other (see Scheme S-2), indicating equal distribution of charge density everywhere in 3-membered moiety of $B_3^-$. By removing all the electrons from valence shell of $B_3^-$, charge density of critical points decreases and all (3, −3) critical points except (3, −3) critical points coinciding with boron atoms vanish and a topological ring forms in which the ratio of $\rho(3, -1)/\rho(3, +1)$ is equal to 3.3947 (for the cluster that contains all its K shell electrons).

The QTAIM and the topological analysis of charge density revealed that electron density in $B_3^-$ is considerably delocalized and distributed over the cluster almost equally, and the valence shell is quite flat everywhere in the frame of molecule, very similar to the valence shell electrons of metals.

## 4. Conclusion

Different criteria of bonding were employed to draw a picture of bonding in $H_3^+$, $Li_3^+$ and $B_3^-$. Electron densities of critical points in

Please cite this article in press as: C. Foroutan-Nejad, P. Rashidi-Ranjbar, J. Mol. Struct. (THEOCHEM) (2009), doi:10.1016/j.theochem.2009.02.003

the topology of charge density demonstrate that charge density is very flat in all species. Studying the effects of individual MOs on charge density revealed that valence electrons in $Li_3^+$ and $B_3^-$ are responsible for flatness of charge density; similar to free electrons in metallic species.

Topological networks in $H_3^+$ and $B_3^-$ are unstable as they are sensitive to nuclear excursions, but MG of $Li_3^+$ is stable under finite geometry changes. The ratio of $\rho(3, -3)/\rho(3, -1)$ indicates that electron density of $Li_3^+$ is less flat compared to $H_3^+$ and $B_3^-$.

The delocalization indices derived from the QTAIM calculations are used to draw the lines for defining the molecular structure since delocalization indices are unique indicator of covalent bonding [17], and according to chemical traditions only covalent bonds are depicted by solid lines to build up molecular structure.

$H_3^+$ could be depicted as a 3-membered ring with three hydrogen atoms at the edges of the triangle as delocalization between basins of hydrogen atoms is higher than delocalization between basin of pseudo atom and the basin of each hydrogen atom.

In $Li_3^+$, covalent bonds are not present; three lithium atoms have surrounded a part of their free valence electrons which is manifested as a pseudo atom in topology of charge density of $Li_3^+$. Electrons in the basin of pseudo atom in $Li_3^+$ are less stabilized compared to $H_3^+$ and $B_3^-$, this is evident by considering energy of electrons in basin of pseudo atoms in three species, Table 2, and more precisely by studying the energy per electron, E ($\Omega$)/N ($\Omega$), in basin of pseudo atoms in $H_3^+$, $Li_3^+$ and $B_3^-$. Electrons in the basin of pseudo atom in $Li_3^+$ are best described as metallic free electrons, regarding their low energy, large volume of the pseudo atom and their topological stability toward nuclear excursions. $Li_3^+$ is suggested to be the lightest tri-atomic molecule with metallic bonding. We propose that MG obtained from topological analysis of charge density is the most satisfactory representation of molecular structure for this molecule.

$B_3^-$ is evidently covalently bonded but regarding the floppy nature of charge density, covalent bonds in this molecule seem to be non-directional. It is demonstrated that MG of $B_3^-$ changes by nuclear motions (this situation has been observed in $B_6C^{2-}$ as well [45,50]); moreover electron density in $B_3^-$ is very flat. It seems that a simple 3-membered structure is incapable for depicting molecular structure of $B_3^-$, even if one neglects molecular motions. On the other hand, MG obtained from topological analysis of charge density which shows only the connection between boron atoms and NNM is also insufficient for representing molecular structure of $B_3^-$, since the delocalization between boron atoms is comparable with the delocalization between basins of these atoms and the basin of pseudo atom in the center of molecule. Although the electrons in basin of pseudo atom in $B_3^-$ are not as free as the electrons in basin of pseudo atom in $Li_3^+$ (by comparing volume, volume per electron, energy and energy per electron in both species), the floppy nature of charge density in $B_3^-$ suggests a kind of metallic bonding in this molecule.

## Acknowledgments

We thank Dr. S. Shahbazian for his helpful discussions. We are grateful to Prof. S.W. Ng for making us available his software (G98w) and hardware (computational time) facilities. We also acknowledge Dr. G.H. Shafiee for making us available the AIM 2000 software.

## Appendix A. Supplementary data

Supplementary data associated with this article can be found, in the online version, at doi:10.1016/j.theochem.2009.02.003.

## References

[1] R.F.W. Bader, Atoms in Molecules: A Quantum Theory, Oxford University Press, Oxford, UK, 1990.
[2] R.F.W. Bader, Chem. Rev. 91 (1991) 893.
[3] C. Gatti, P. Fantucci, G. Pacchioni, Theor. Chim. Acta 72 (1987) 433.
[4] W.L. Cao, C. Gatti, P.J. MacDougall, R.F.W. Bader, Chem. Phys. Lett. 141 (1987) 380.
[5] C. Mei, K.E. Edgecombe, V.H. Smith, A. Heilingbrunner, Int. J. Quantum Chem. 48 (1993) 287.
[6] K.E. Edgecombe, R.O. Esquivel, V.H. Smith, F.J. Müller-Plathe, J. Chem. Phys. 97 (1992) 2593.
[7] B.B. Iversen, F.K. Larsen, M. Souhassou, M. Takata, Acta Crystallogr. Sect. B: Struct. Sci. 51 (1995) 580.
[8] R.Y. de Vries, W.J. Briels, D. Feil, Phys. Rev. Lett. 77 (1996) 1719.
[9] B.B. Iversen, J.L. Jensen, J. Danielsen, Acta Crystallogr. Sect. A Found. Crystallogr. 53 (1997) 376.
[10] D. Jayatilaka, Phys. Rev. Lett. 80 (1998) 798.
[11] R.F.W. Bader, J.A. Platts, J. Chem. Phys. 107 (1997) 8545.
[12] G.K.H. Madsen, C. Gatti, B.B. Iversen, L.j. Damjanovic, G.D. Stucky, V.I. Srdanov, Phys. Rev. B 59 (1999) 12359.
[13] V. Luana, P. Mori-Sanchez, A. Costales, M.A. Blanco, A.M. Pendas, J. Chem. Phys. 119 (2003) 6341.
[14] F. Cortes-Guzman, R.F.W. Bader, Coord. Chem. Rev. 249 (2005) 633.
[15] M.J. Frisch, G.W. Trucks, H.B. Schlegel, G.E. Scuseria, M.A. Robb, J.R. Cheeseman, V.G. Zakrzewski, J.A. Montgomery Jr., R.E. Stratmann, J.C. Burant, S. Dapprich, J.M. Millam, A.D. Daniels, K.N. Kudin, M.C. Strain, O. Farkas, J. Tomasi, V. Barone, M. Cossi, R. Cammi, B. Mennucci, C. Pomelli, C. Adamo, S. Clifford, J. Ochterski, G.A. Petersson, P.Y. Ayala, Q. Cui, K. Morokuma, D.K. Malick, A.D. Rabuck, K. Raghavachari, J.B. Foresman, J. Cioslowski, J.V. Ortiz, B.B. Stefanov, G. Liu, A. Liashenko, P. Piskorz, I. Komaromi, R. Gomperts, R.L. Martin, D.J. Fox, T. Keith, M.A. Al-Laham, C.Y. Peng, A. Nanayakkara, C. Gonzalez, M. Challacombe, P.M.W. Gill, B. Johnson, W. Chen, M.W. Wong, J.L. Andres, C. Gonzalez, M. Head-Gordon, E.S. Replogle, J.A. Pople, Gaussian 98, Revision A.6, Gaussian, Inc., Pittsburgh, PA, 1998.
[16] (a) F.W. Biegler-König, J. Schönbohm, J. Comput. Chem. 23 (2002) 1489; (b) F.W. Biegler-König, J. Schönbohm, D. Bayles, J. Comput. Chem. 22 (2001) 545.
[17] L.J. Farrugia, C. Evans, M. Tegel, J. Phys. Chem. A 110 (2006) 7952.
[18] J.J. Thomson, Phil. Mag. 21 (1911) 225.
[19] J.J. Thomson, Phil. Mag. 24 (1912) 209.
[20] C.A. Coulson, Proc. Camb. Phil. Soc. 31 (1935) 244.
[21] E. Herbest, W. Klemperer, Astrophys. J. 185 (1973) 505.
[22] W.D. Watson, Astrophys. J. 183 (1973) L17.
[23] W.D. Watson, Rev. Mood. Phys. 48 (1976) 513.
[24] T. Oka, Phys. Rev. Lett. 45 (1980) 531.
[25] T. Oka, Rev. Mod. Phys. 64 (1992) 1141.
[26] T.R. Geballe, T. Oka, Nature 384 (1996) 334.
[27] T. Oka, Phil. Trans. R. Soc. A 358 (2000) 2363 (for Corrigendum see: Phil. Trans. R. Soc. A 364 (2006) 3149).
[28] B.J. McCall, Phil. Trans. R. Soc. A 358 (2000) 2385.
[29] J. Tennyson, S. Miller, Spectrochim. Acta A 57 (2001) 661.
[30] T. Oka, Proc. Nat. Acad. Sci. (PNAS) 103 (2006) 12235.
[31] B.J. McCall, Nature 440 (2006) 157.
[32] G.D. Carney, R.N. Porter, J. Chem. Phys. 60 (1974) 4251.
[33] G.D. Carney, R.N. Porter, J. Chem. Phys. 65 (1976) 3547.
[34] R.N. Porter, Ber. Bunsenges. Phys. Chem. 86 (1982) 407.
[35] W. Meyer, P. Botschwina, P. Burton, J. Chem. Phys. 84 (1986) 891.
[36] R. Röhse, W. Klopper, W. Kutzelnigg, J. Chem. Phys. 99 (1993) 8830.
[37] R. Röhse, W. Kutzelnigg, R. Jaquet, W. Klopper, J. Chem. Phys. 101 (1994) 2231.
[38] W. Cencek, J. Rychlewski, R. Jaquet, W. Kutzelnigg, J. Chem. Phys. 108 (1998) 2831.
[39] R. Jaquet, W. Cencek, W. Kutzelnigg, J. Rychlewski, J. Chem. Phys. 108 (1998) 2837.
[40] O.L. Polyansky, J. Tennyson, J. Chem. Phys. 110 (1999) 5056.
[41] R.F.W. Bader, S.G. Anderson, A.J. Duke, J. Am. Chem. Soc. 101 (1979) 1389.
[42] R.F.W. Bader, T.T. Nguyen-Dang, Y. Tal, J. Chem. Phys. 70 (1979) 4316.
[43] A. Sadjadi, M. Abdzadeh, H. Behnejad, J. Chem. Res. 5 (2004) 358.
[44] R.W.A. Havenith, F. De Proft, P.W. Fowler, P. Geerlings, Chem. Phys. Lett. 407 (2005) 391.
[45] C. Foroutan-Nejad, G.H. Shafiee, A. Sadjadi, S. Shahbazian, Can. J. Chem. 84 (2006) 771.
[46] G.K.H. Madsen, P. Blaha, K. Schwarz, J. Chem. Phys. 117 (2002) 8030.
[47] A.N. Alexandrova, A.I. Boldyrev, J. Phys. Chem. A 107 (2003) 554.
[48] A.E. Kuznetsov, A.I. Boldyrev, Struct. Chem. 13 (2002) 2.
[49] H.J. Zhai, L.S. Wang, A.N. Alexandrova, A.I. Boldyrev, V.G. Zakrzewski, J. Phys. Chem. A 107 (2003) 9319.
[50] Sh. Shahbazian, A. Sadjadi, THEOCHEM 822 (2007) 116.